0026-895X/05/6705-1655–1665$20.00
MOLECULAR PHARMACOLOGY

Mol Pharmacol 67:1655–1665, 2005

Vol. 67, No. 5
8615/1198150
Printed in U.S.A.

Pharmacological Discrimination of Calcitonin Receptor: Receptor Activity-Modifying Protein Complexes

Debbie L. Hay, George Christopoulos, Arthur Christopoulos, David R. Poyner, and Patrick M. Sexton

School of Biological Sciences, University of Auckland, Auckland, New Zealand (D.L.H.); Howard Florey Institute (G.C., P.M.S.) and Department of Pharmacology (A.C.), University of Melbourne, Victoria, Australia; and School of Life and Health Sciences, Aston University, Birmingham, United Kingdom (D.R.P.)

Received October 21, 2004; accepted February 3, 2005

ABSTRACT

Calcitonin (CT) receptors dimerize with receptor activity-modifying proteins (RAMPs) to create high-affinity amylin (AMY) receptors, but there is no reliable means of pharmacologically distinguishing these receptors. We used agonists and antagonists to define their pharmacology, expressing the $CT_{(a)}$ receptor alone or with RAMPs in COS-7 cells and measuring cAMP accumulation. Intermedin short, otherwise known as adrenomedullin 2, mirrored the action of αCGRP, being a weak agonist at $CT_{(a)}$, $AMY_{2(a)}$, and $AMY_{3(a)}$ receptors but considerably more potent at $AMY_{1(a)}$ receptors. Likewise, the linear calcitonin gene-related peptide (CGRP) analogs $(Cys(ACM)^{2,7})$hαCGRP and $(Cys(Et)^{2,7})$hαCGRP were only effective at $AMY_{1(a)}$ receptors, but they were partial agonists. As previously observed in COS-7 cells, there was little induction of the $AMY_{2(a)}$ receptor phenotype; thus, $AMY_{2(a)}$ was not examined further in this study. The antagonist peptide salmon $calcitonin_{8-32}$ (sCT_{8-32}) did not discriminate strongly between CT and AMY receptors; however, AC187 was a more effective antagonist of AMY responses at AMY receptors, and AC413 additionally showed modest selectivity for $AMY_{1(a)}$ over $AMY_{3(a)}$ receptors. $CGRP_{8-37}$ also demonstrated receptor-dependent effects. $CGRP_{8-37}$ more effectively antagonized AMY at $AMY_{1(a)}$ than $AMY_{3(a)}$ receptors, although it was only a weak antagonist of both, but it did not inhibit responses at the $CT_{(a)}$ receptor. Low $CGRP_{8-37}$ affinity and agonism by linear CGRP analogs at $AMY_{1(a)}$ are the classic signature of a $CGRP_2$ receptor. Our data indicate that careful use of combinations of agonists and antagonists may allow pharmacological discrimination of $CT_{(a)}$, $AMY_{1(a)}$, and $AMY_{3(a)}$ receptors, providing a means to delineate the physiological significance of these receptors.

The peptides typically designated as calcitonin (CT) peptide family members include CT gene-related peptide (CGRP), amylin (AMY), and adrenomedullin (AM) (Poyner et al., 2002), although an assortment of related peptides has recently been identified, including intermedin (IMD), also known as AM2 (Katafuchi et al., 2003; Roh et al., 2004; Takei et al., 2004). Although only weakly homologous in terms of amino acid sequence, several common features are shared, including an N-terminal ring structure that is the key to agonist activity. Nonetheless, the similarity in peptide structure leads to promiscuity for many of these peptides across their cognate receptors. Numerous biological activities have been attributed to these peptides. CT, for example, is involved in bone homeostasis (Sexton et al., 1999). AMY is likely to be involved in nutrient intake and regulating blood glucose levels (Cooper, 1994). CGRP and AM are both potent vasodilators, with AM necessary for vascular integrity (Hinson et al., 2000; Shindo et al., 2001; Brain and Grant, 2004). As with many other peptides, significant advances in understanding the physiological, pathophysiological, and clinical potential of CT family members are hampered by a lack of selective pharmacological agents that can be used to define function. Progress has been particularly slow for the CT peptide family because, until recently, the

This work was supported by the National Health and Medical Research Council of Australia (grants 145702 and 299810), the Ian Potter Foundation Neuropeptide Laboratory and the University of Auckland Staff Research Fund, the Auckland Medical Research Foundation, and Lottery Health Commission (New Zealand). P.M.S. and A.C. are Senior Research Fellows of the National Health and Medical Research Council. D.R.P. was supported by the British Heart Foundation (Grant PG/03/079/15278).

Article, publication date, and citation information can be found at http://molpharm.aspetjournals.org.

doi:10.1124/mol.104.008615.

ABBREVIATIONS: CT, calcitonin; CGRP, calcitonin gene-related peptide; AMY, amylin; AM, adrenomedullin; IMD, intermedin; GPCR, G protein coupled receptor; CL, calcitonin receptor-like receptor; RAMP, receptor activity modifying protein; $CT_{(a)}$, calcitonin receptor; rAMY, rat amylin; IMDS, intermedin short; BSA, bovine serum albumin; ALPHA, amplified luminescent proximity homogenous assay; DMEM, Dulbecco's modified Eagle's medium; FBS, fetal bovine serum; HA, hemagglutinin; PBS, phosphate-buffered saline; hCT, human calcitonin; AC187, SC[acetyl-

molecular nature of the cognate receptors for AMY, CGRP, and adrenomedullin was unknown.

There is now some clarity regarding the nature of the receptor that probably mediates many of the effects of CGRP. It consists of a complex between a seven-transmembrane protein belonging to the secretin family of G protein-coupled receptors (GPCRs), the CT receptor-like receptor (CL), with receptor activity modifying protein (RAMP)1 (McLatchie et al., 1998). When these proteins are coexpressed, classic $CGRP_1$-like pharmacology is observed (McLatchie et al., 1998; Hay et al., 2004). However, if CL is instead coexpressed with either of the two other RAMP family members, RAMP2 or RAMP3, adrenomedullin is recognized most effectively (McLatchie et al., 1998). Thus, RAMPs act as pharmacological switches. It was soon realized that the function of RAMPs may be much broader, and there are now several examples of secretin family GPCRs with which these proteins are likely to interact (Christopoulos et al., 1999, 2003; Leuthauser et al., 2000).

It is noteworthy that RAMPs have a strong interaction with the CT receptor, the closest relative to CL (Christopoulos et al., 1999). Together, RAMPs and the CT receptor generate receptors with high affinity for AMY, with the precise nature of these receptors depending on the CT receptor splice variant and cellular background (Tilakaratne et al., 2000). To our knowledge, there have been no other reports of a distinct molecular entity capable of responding to AMY with such high affinity. It is noteworthy that early attempts to clone the AMY receptor usually produced the CT receptor; thus, it is likely that CT receptor/RAMP complexes mediate at least some of the effects of AMY in vivo, although this has yet to be directly tested. It is crucial to note that there is no reliable means of distinguishing CT from AMY receptors or AMY receptor subtypes pharmacologically in functional systems. Although comprehensive binding and agonist-interaction analyses have been performed, there has been no critical analysis of the way that antagonists interact with these receptors. This type of information may allow the different biological effects of AMY and related peptides to be attributed to distinct receptor subtypes. It can also provide a basis for the rational design of more selective agents. This is important because an AMY analog (Pramlintide) has now reached late-stage development for glycemic control in diabetic patients, illustrating the clinical importance of this peptide.

Therefore, in this study, we have sought to address this issue by transfecting the CT receptor [$CT_{(a)}$; Poyner et al., 2002] with or without RAMPs into COS-7 cells that do not endogenously express phenotypically significant levels of RAMPs, CT receptors, or CL. We have identified several key aspects of pharmacology that relate to the way that AMY and its related peptides have historically been reported to act in tissues.

Materials and Methods

Materials. Human AM, human adrenomedullin$_{22\text{-}52}$ ($AM_{22\text{-}52}$), rat $AMY_{8\text{-}37}$, human αCGRP, human $\alpha CGRP_{8\text{-}37}$, human βCGRP, and acetyl-(Asn^{30},Tyr^{32})-calcitonin$_{8\text{-}32}$ (AC187) were purchased from Bachem (Bubendorf, Switzerland). Salmon calcitonin$_{8\text{-}32}$ [$sCT_{8\text{-}32}$] was from Peninsula Laboratories (Belmont, CA), and human $Tyr^0\alpha$CGRP, $(Cys(Et)^{2,7})$-αCGRP, $(Cys(Acm)^{2,7})$-αCGRP, and rat AMY (rAMY) were from Auspep (Parkville, Australia). AC413 was a La Jolla, CA). Human CT was obtained from the American Peptide Co., Inc. (Sunnyvale, CA). IMD short (IMDS) was a generous gift from Dr. Teddy Hsu (Stanford University School of Medicine, Stanford, CA; Roh et al., 2004). Peptide sequences are detailed in Fig. 1. Bovine serum albumin (BSA) and 3-isobutyl-1-methylxanthine were from Sigma-Aldrich (St. Louis, MO), and amplified luminescent proximity homogenous assay (ALPHA)-screen cAMP kits were purchased from PerkinElmer Life and Analytical Sciences (Boston, MA). Dulbecco's modified Eagle's medium (DMEM), fetal bovine serum (FBS), and HEPES were from Invitrogen (Carlsbad, CA). Cell culture plastic ware was manufactured by NUNC A/S (Roskilde, Denmark), and Metafectene was purchased from Scientifix (Cheltenham, VIC, Australia). ^{125}I-Labeled goat anti-mouse IgG was obtained from PerkinElmer Life and Analytical Sciences. Na-^{125}I (100 mCi/ml) was supplied by MP Biomedicals (Irvine, CA). ^{125}I-Salmon CT (specific activity, 700 Ci/mmol) was iodinated in-house as described previously (Findlay et al., 1980). *N*-Succinimidyl 3-94-hydroxy,5,-[^{125}I]iodophenyl propionate (Bolton-Hunter reagent; 2000 Ci/mmol) was from Amersham Biosciences UK, Ltd. (Little Chalfont, Buckinghamshire, UK). ^{125}I-Rat amylin (specific activity, 2000 Ci/mmol) was iodinated by the Bolton-Hunter method and purified by reverse phase high-performance liquid chromatography as described previously (Bhogal et al., 1992). All other reagents were of analytical grade.

Expression Constructs. Double hemagglutinin (HA) epitope-tagged human $CT_{(a)}$ receptor was prepared as described previously (Pham et al., 2004). This receptor is the Leu^{447} polymorphic variant of the receptor (Kuestner et al., 1994). Human RAMP1, RAMP2, and RAMP3 and human CL receptor were a gift from Dr. Steven Foord (McLatchie et al., 1998).

Cell Culture and Transfection. COS-7 cells were subcultured as described previously (Zumpe et al., 2000). One day before transfection, COS-7 cells were seeded into 25- or 75-cm^2 cell culture flasks at high density to achieve 90 to 100% confluence for transfection the next day. The cells were then transfected using Metafectene according to the manufacturer's instructions, with the following amounts of DNA: For 25-cm^2 flasks, 1.25 μg of receptor DNA [$CT_{(a)}$ or CL] and 1.9 μg of RAMP or pcDNA3 DNA; for 75-cm^2 flasks, 3.8 μg of receptor DNA, and 5.7 μg of RAMP or pcDNA3 DNA. The transfection mix was removed after 16-h incubation, and the cells were recovered in complete media (DMEM with 5% FBS) for 8 h. The cells were then serum-starved for a further 16 h to minimize basal cAMP levels.

Measurement of cAMP Production. Cells transfected with $CT_{(a)}$ or CL plus pcDNA3, RAMP1, -2, or -3 were harvested approximately 40 h after transfection. The cells were counted and diluted to 20,000 cells per 10 μl and incubated, mixing for at least 30 min in serum and phenol red-free DMEM containing 0.1% (w/v) BSA and 1 mM 3-isobutyl-1-methylxanthine (stimulation buffer). Agonist and antagonist dilutions were prepared in stimulation buffer and added to white 384-well plates, either alone or in combination, to a total volume of 10 μl. After incubation of cells with stimulation buffer, 20,000 cells were added per well in a volume of 10 μl. The plates were centrifuged very briefly to ensure thorough mixing of these small volumes. The plates were then incubated for 30 min at 37°C. Drug-stimulated receptor activity was terminated by the addition of 20 μl of lysis buffer [0.3% (v/v) Tween 20, 5 mM HEPES, 0.1% (w/v) BSA in water, pH 7.4]. After addition of lysis buffer, the plates were again centrifuged briefly to ensure thorough mixing. The cAMP in the lysed cells was assayed in the same wells using ALPHA-screen assay kits. A cAMP standard curve was included in each assay. In brief, cAMP was measured with acceptor and donor beads that were prepared in lysis buffer and added to the plates according to the manufacturer's instructions. After overnight incubation in the dark, the plates were read with an ALPHA-screen protocol on a Fusion plate reader (PerkinElmer Life and Analytical Sciences).

Radioligand Binding. When harvested for cAMP assay (see above), the same transfected COS-7 cells were also seeded into 24-

well. These cells were then assayed for receptor binding to either ^{125}I-rAMY or ^{125}I-sCT the next day (16 h later). Cells were initially washed with 500 μl of phosphate-buffered saline (PBS) and incubated for 30 min at 37°C in 500 μl of binding buffer [FBS-free DMEM with 0.1% (w/v) BSA]. Wells contained either 50 pM ^{125}I-sCT or 100 pM ^{125}I-rAMY. Nonspecific binding levels were determined by competing with 10^{-7} M sCT or 10^{-6} M rAMY, respectively. Cells were then washed twice with 500 μl of PBS and were solubilized with 0.5 ml of 0.5 M NaOH with the cell lysate counted for γ-radiation using a PerkinElmer γ-counter (COBRA Auto-gamma, Model B5010; 75% efficiency).

For full-curve competition binding experiments, cells in 75-cm^2 flasks were transfected for 5 h using Metafectene, with 3.7 μg of $CT_{(a)}$ and either 5.2 μg of pcDNA3, RAMP1, or RAMP3 DNA. The cells were allowed to recover for 16 h and then harvested and seeded at around 80 to 90% confluence into 48-well plates. These were then allowed to adhere and recover for a further 16 h. Competition binding was performed for 2 h at room temperature. Each well contained 225 μl of DMEM + 0.1% BSA, 200 pM ^{125}I-rAMY, and 25 μl of competing peptide (10^{-12}–10^{-7} M) or buffer control. Cells were washed once with PBS, lysed, and counted as described above.

Measurement of Cell Surface Expression by Antibody Binding. As for binding assays, at the time of harvesting for cAMP assay, transfected COS-7 cells were plated into 24-well plates and later assayed for cell-surface expression of the HA-tagged receptor. Cells were rinsed twice with 0.5 ml of binding buffer [50 mM Tris-HCl, pH 7.7, 100 mM NaCl, 5 mM KCl, 2 mM $CaCl_2$, and 1% (w/v) BSA, adjusted to pH 7.7 with HCl] followed by addition of 2 μg of HA-specific mouse antibody in 250 μl of binding buffer to each well. Cells were incubated for 3 h at 4°C, with gentle agitation. Cells were then rinsed three times with binding buffer, and ^{125}I-labeled goat anti-mouse IgG (diluted to give 200 pM/250 μl per well) was added to the cells. The cells were incubated for a further 3 h at 4°C and then rinsed three times with binding buffer. Cells were solubilized with 0.5 ml of 0.5 M NaOH, and the cell lysate was counted for γ-radiation. Nonspecific binding was determined from the wells that received ^{125}I-labeled goat anti-mouse IgG but not the anti-HA primary antibody.

Data Analysis and Statistics. Data were analyzed using Prism 4.02 (GraphPad Software Inc., San Diego, CA). In each assay, the quantity of cAMP generated was calculated from the raw data using a cAMP standard curve. For agonist responses, concentration-effect curves were fitted to a four-parameter logistic equation (Motulsky and Christopoulos, 2003).

For calculation of antagonist potency, agonist concentration-response curves in the absence and presence of antagonist were globally fitted to the following equation using Prism (Motulsky and Christopoulos, 2004):

$$\text{Response} = E_{\min} + \frac{(E_{\max} - E_{\min})[A]^{n_H}}{[A]^{n_H} + \left(10^{-\text{pEC}_{50}}\left[1 + \left(\frac{[B]}{10^{-\text{pA}_2}}\right)^{s}\right]\right)^{n_H}}$$

where E_{max} represents the maximal asymptote of the concentration-response curves, E_{min} represents the lowest asymptote of the concentration-response curves, pEC_{50} represents the negative logarithm of the agonist EC_{50} in the absence of antagonist, [A] represents the concentration of the agonist, [B] represents the concentration of the antagonist, n_H represents the Hill slope of the agonist curve, s represents the Schild slope for the antagonist, and pA_2 represents

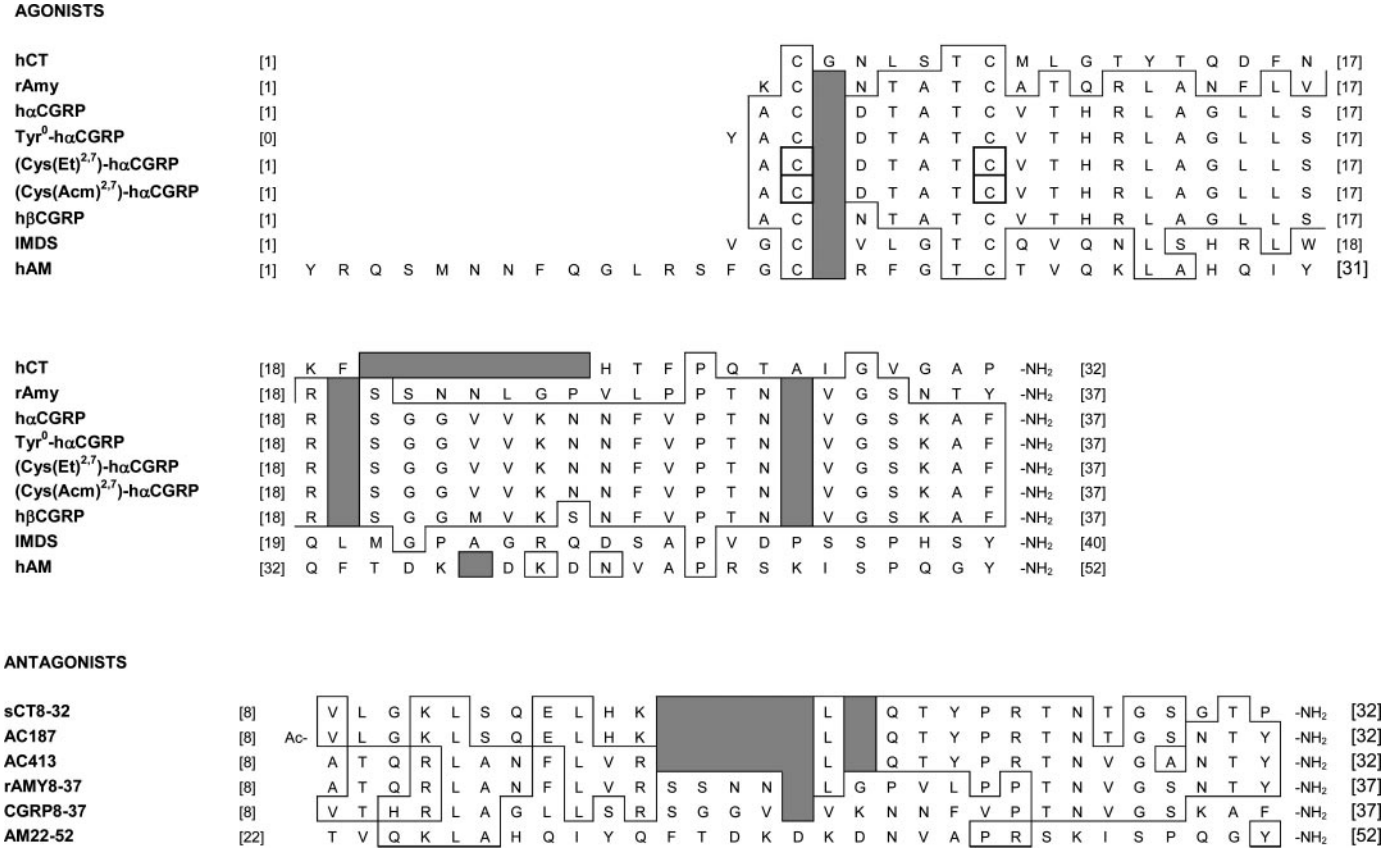

Fig. 1. Peptide sequences and alignment. Sequences were aligned according to the ClustalV methods (PAM250) using the MegAlign program from DNAstar Inc. (Madison, WI). For agonist peptides, residues that match the consensus CGRP sequence are boxed (top). For antagonist peptides, residues that match the overall consensus are boxed (bottom). The location of the disulfide-linked cysteines in agonist peptides is also indicated. The exception to this are the analogs Cys(Et)^{2,7}-αCGRP and Cys(Acm)^{2,7}-αCGRP where the disulfide linkage has been blocked. Modification to these

the negative logarithm of the concentration of antagonist that shifts the agonist EC_{50} by a factor of 2. Parallelism of agonist concentration-response curves in the presence of antagonist relative to the absence of antagonist was assessed by F-test, which compared curve fits where the n_H parameter was shared across each family of curves to fits where each curve within a family was allowed its own Hill slope factor. The F-test was similarly used to determine whether the Schild slope was significantly different from unity within a given data set. In the majority of instances, this was not the case, and thus all curves were refitted with the Schild slope constrained to a value of 1; under these conditions, the resulting estimate of pA_2 represents the pK_B.

In all cases, potency and affinity values were estimated as logarithms (Christopoulos, 1998). Data shown are the mean ± S.E.M. Comparisons between mean values were performed by unpaired *t* tests or one-way analysis of variance, as appropriate. Unless otherwise stated, values of $p < 0.05$ were taken as statistically significant.

Results

COS-7 cells were chosen for transfection studies as they have been shown to lack phenotypically significant levels of endogenous RAMPs, CT receptors, and CL (Hay et al., 2003). Without significant background expression of such receptor components, defined receptor subtypes can be accurately compared.

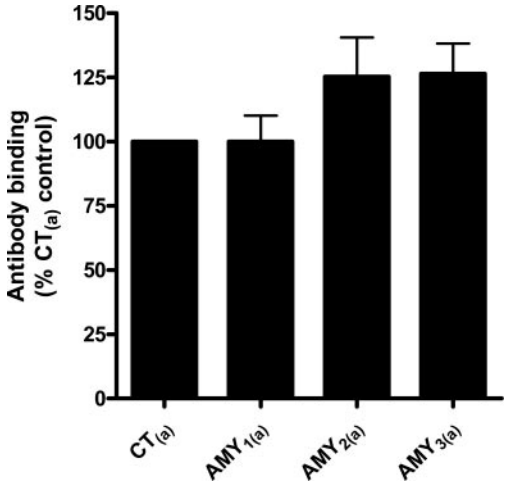

Fig. 2. Cell surface expression of $CT_{(a)}$ protein, in COS-7 cells transiently transfected with $CT_{(a)}$ alone or $CT_{(a)}$ in the presence of either RAMP1 [$AMY_{1(a)}$], RAMP2 [$AMY_{2(a)}$], or RAMP3 [$AMY_{3(a)}$], measured by binding of anti-HA antibody to the 2xHA epitope incorporated at the N terminus of the receptor. Primary antibody binding is detected by incubation of a ^{125}I-labeled goat anti-mouse IgG antibody as described under *Materials and Methods*. In untransfected or mock-transfected cells the level of binding was <15% of binding seen in $CT_{(a)}$-transfected cells. Data are expressed as a percentage of the binding of ^{125}I-antibody to cells expressing the $CT_{(a)}$ protein in the absence of RAMP cotransfection. Data are from 10 independent experiments with duplicate repeats.

Agonist Pharmacology. The approach taken to generate a detailed pharmacological analysis of the molecularly defined AMY receptors was to compare the effects of all available antagonists against the major agonists that were capable of eliciting reliable receptor activation. Therefore, we initially examined agonist-induced cAMP responses in cells transfected with $CT_{(a)}$ alone or in combination with individual RAMPs to assess the relative agonist activation profiles of the receptors defined as $CT_{(a)}$, $AMY_{1(a)}$, $AMY_{2(a)}$, and $AMY_{3(a)}$, respectively. In most experiments, cell surface expression of the $CT_{(a)}$ was confirmed by binding of an anti-HA antibody to the epitope tag incorporated into the N terminus of the receptor (Fig. 2). In addition, in some experiments ^{125}I-sCT binding was also performed and confirmed that similar levels of the receptor protein were expressed at the cell surface (data not shown). Expression of the AMY receptor phenotype was confirmed by concomitant ^{125}I-rAMY binding (data not shown).

As shown in Table 1 and in accordance with previous results, hCT displayed equivalent high potency in cells transfected with $CT_{(a)}$ or $AMY_{1(a)}$ receptors but had ~10-fold lower potency at $AMY_{3(a)}$ receptors ($p < 0.05$; $n = 6$). In contrast, rAMY and the CGRPs had low potency at the $CT_{(a)}$ receptor and exhibited ~100-fold increased potency at the $AMY_{1(a)}$ receptor. As seen previously in this cellular background, preliminary analysis of radioligand binding and cAMP response indicated very little induction of $AMY_{2(a)}$ phenotype with pEC_{50} values for rAMY at this receptor equivalent to that seen with $CT_{(a)}$ alone (data not shown; Christopoulos et al., 1999; Tilakaratne et al., 2000). rAMY had high potency at the $AMY_{3(a)}$ receptor, but the CGRPs showed only modest increases in potency (<10-fold) at this receptor. At all receptor phenotypes, Tyr^0-hαCGRP was weaker than unmodified hαCGRP, but it exhibited similar modulation of potency to α- and β-CGRP at $AMY_{1(a)}$ receptors.

IMD displays efficacy at CL/RAMP-based receptors (Roh et al., 2004; Takei et al., 2004). We examined the interaction of the short form of this peptide, IMDS, with CT and AMY receptors and compared it with the behavior of the peptide at CGRP and AM receptors. IMDS had low potency at $CT_{(a)}$ and $AMY_{2(a)}$ receptors and displayed a similar increase in potency at $AMY_{1(a)}$ (~40-fold) and $AMY_{3(a)}$ (<10 fold) receptors,

TABLE 1

Agonist potencies (pEC_{50} values) for stimulation of cAMP accumulation at human CT and AMY receptors

Data are presented as mean ± S.E.M. Values in parentheses represent the number of individual experiments analyzed.

	$CT_{(a)}$	$AMY_{1(a)}$	$AMY_{3(a)}$
hCT	8.99 ± 0.1 (8)	8.93 ± 0.09 (7)	8.02 ± 0.22 (7)
rAMY	6.95 ± 0.18 (8)	9.12 ± 0.16 (10)	8.63 ± 0.09 (7)
hαCGRP	6.80 ± 0.05 (5)	8.70 ± 0.17 (6)	7.60 ± 0.17 (6)
Tyr^0-hαCGRP	<6 (2)	7.55 ± 0.17 (7)	<6 (3)
hβCGRP	7.18 ± 0.22 (2)	9.16 ± 0.18 (9)	7.67 ± 0.23 (6)
$(Cys(Et)^{2,7})$hαCGRP	<6 (3)	7.79 ± 0.14 (5)[a]	<6 (6)
$(Cys(ACM)^{2,7})$hαCGRP	<6 (3)	7.46 ± 0.06 (4)[a]	<6 (6)
hAM	6.73 ± 0.45 (3)	6.48 ± 0.28 (4)	6.89 ± 0.51 (3)
IMDS	6.53 ± 0.09 (6)	8.07 ± 0.19 (6)[b]	7.12 ± 0.19 (6)

[a] Note that these CGRP analogues were weak partial agonists at this receptor, with E_{max} values of 47.9 ± 5.4 and 22.8 ± 6% for $(Cys(Et)^{2,7})$hαCGRP and $(Cys(ACM)^{2,7})$hαCGRP, respectively. These values were generated by comparing the curve maximum asymptotes of the hαCGRP analogs with that for hαCGRP itself (set at 100%), which was used as the reference full agonist for these experiments.

as seen for the CGRPs (Fig. 3; Table 2). This contrasts with the interaction of IMDS at CGRP and AM receptors assayed in the same cellular background where IMDS displayed similar high efficacy at all three receptors but differed from the activity of hαCGRP at these receptors, which only had high potency at the $CGRP_1$ receptor (Fig. 3; Table 2).

The linear CGRP analogs $(Cys(Et)^{2,7})$-αCGRP and $(Cys(Acm)^{2,7})$-αCGRP have been used to subclassify CGRP receptors into $CGRP_1$ and $CGRP_2$ receptors (Dennis et al., 1990, 1991; Poyner et al., 2002). Because AMY receptors can also function as high-affinity CGRP receptors, it was of interest to assess the potency of the linear CGRP analogs at CT and AMY receptors. Both analogs had very low potency and efficacy at $CT_{(a)}$, $AMY_{2(a)}$, and $AMY_{3(a)}$ receptors, but they displayed moderate potency at the $AMY_{1(a)}$ receptor (Table 1; Fig. 4A). However, both analogs were only partial agonists at the latter receptor exhibiting $\%E_{max}$ responses of 47.9 ± 5.4 and 22.8 ± 6.0, respectively, for $(Cys(Et)^{2,7})$-αCGRP and $(Cys(Acm)^{2,7})$-αCGRP. At the $CGRP_1$ receptor, both analogs displayed high potency, pEC_{50} of 9.4 ± 0.12 ($n = 5$) and 9.08 ± 0.63 ($n = 4$) for $(Cys(Et)^{2,7})$-αCGRP and $(Cys(Acm)^{2,7})$-αCGRP, respectively, similar to unmodified hαCGRP [9.51 ± 0.14 ($n = 5$)], but they were again partial agonists. However, $(Cys(Et)^{2,7})$-αCGRP was considerably more efficacious than $(Cys(Acm)^{2,7})$-αCGRP with $\%E_{max}$ values of 83.5 ± 7.2 and 8.1 ± 2.1, respectively (Fig. 4B).

TABLE 2
Comparison of IMDS and hαCGRP potency for stimulation of cAMP accumulation at human CT, AMY, CGRP, and AM receptors
Values are presented as mean ± S.E.M.

Receptor	Agonist	pEC_{50}	n
$CT_{(a)}$	IMDS	6.53 ± 0.09	6
	hαCGRP	6.80 ± 0.04	5
$AMY_{1(a)}$	IMDS	8.07 ± 0.19*	6
	hαCGRP	8.70 ± 0.17	10
$AMY_{2(a)}$	IMDS	6.25 ± 0.26	6
	hαCGRP	7.24 ± 0.19	5
$AMY_{3(a)}$	IMDS	7.12 ± 0.19†	6
	hαCGRP	7.60 ± 0.17	6
$CGRP_1$	IMDS	8.71 ± 0.13	8
	hαCGRP	9.47 ± 0.19	6
AM_1	IMDS	8.10 ± 0.04	4
	hαCGRP	6.39 ± 0.10	4
AM_2	IMDS	8.69 ± 0.13	5
	hαCGRP	6.87 ± 0.13	3

* $P < 0.05$ versus $CT_{(a)}$, $AMY_{2(a)}$, and $AMY_{3(a)}$ receptors.
† $P < 0.05$ versus $CT_{(a)}$, $AMY_{1(a)}$, and $AMY_{2(a)}$ receptors.

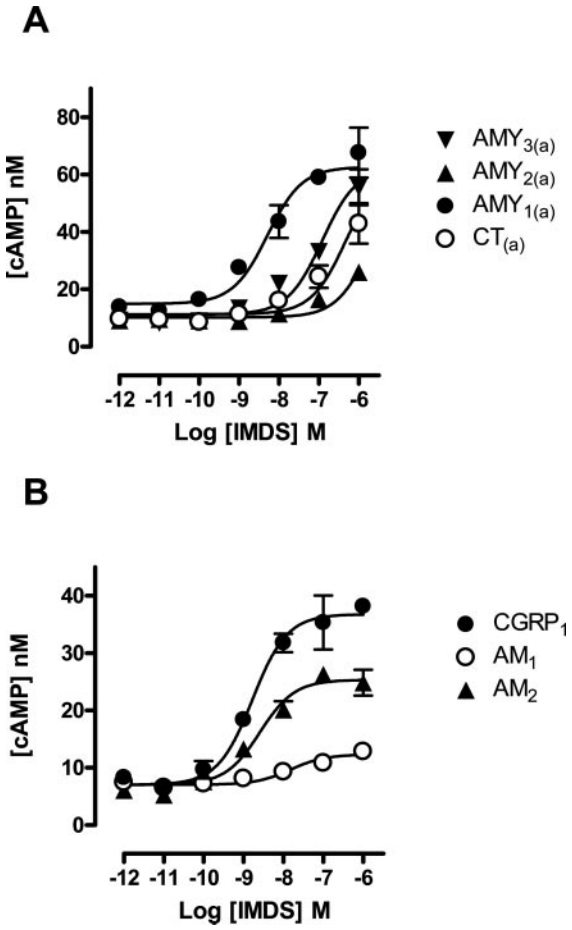

Fig. 3. Induction of cAMP accumulation by IMDS in COS-7 cells transiently transfected with $CT_{(a)}$-based receptor phenotypes (A) and CL-based receptor phenotypes (B). For CGRP and AM receptors, the response across receptors probably represents different levels of receptor expression. The E_{max} for IMDS and hαCGRP was equivalent for all. The graph is of a representative experiment, with triplicate repeats, of at least six

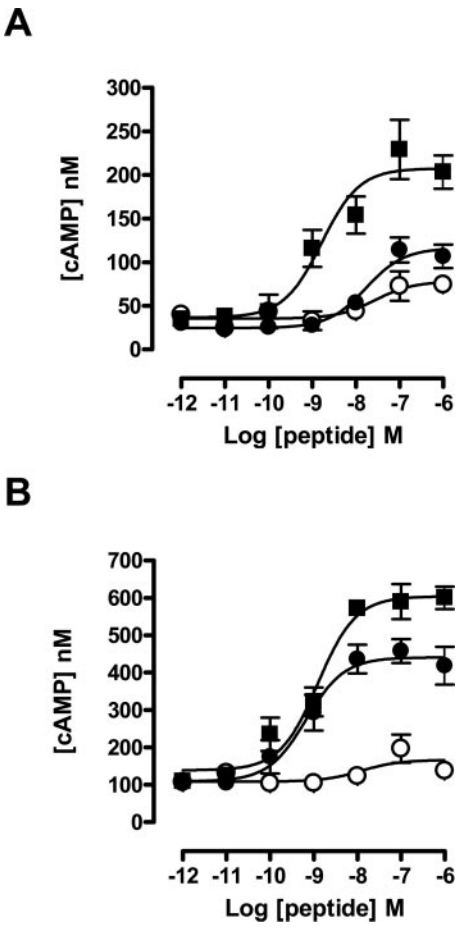

Fig. 4. Induction of cAMP accumulation at $AMY_{1(a)}$ (A) or $CGRP_1$ (B) receptors by linear CGRP analogs. hαCGRP (closed squares), $(Cys(Et)^{2,7})$-αCGRP (●), and $(Cys(Acm)^{2,7})$-αCGRP (open circles). pEC_{50} and E_{max} values, respectively, at the $CGRP_1$ receptor were hαCGRP, 9.51 ± 0.14, 100% ($n = 5$); $(Cys(Et)^{2,7})$-αCGRP, 9.40 ± 0.12, 83.54 ± 7.19% ($n = 5$); and $(Cys(Acm)^{2,7})$-αCGRP, 9.08 ± 0.63, 8.08 ± 2.09% ($n = 4$). The graph is of a representative experiment, with triplicate repeats, of at least four independent experiments. pEC_{50} and E_{max} values for peptides at the

DOCKET ALARM

Explore Litigation Insights

Docket Alarm provides insights to develop a more informed litigation strategy and the peace of mind of knowing you're on top of things.

Real-Time Litigation Alerts

Keep your litigation team up-to-date with **real-time alerts** and advanced team management tools built for the enterprise, all while greatly reducing PACER spend.

Our comprehensive service means we can handle Federal, State, and Administrative courts across the country.

Advanced Docket Research

With over 230 million records, Docket Alarm's cloud-native docket research platform finds what other services can't. Coverage includes Federal, State, plus PTAB, TTAB, ITC and NLRB decisions, all in one place.

Identify arguments that have been successful in the past with full text, pinpoint searching. Link to case law cited within any court document via Fastcase.

Analytics At Your Fingertips

Learn what happened the last time a particular judge, opposing counsel or company faced cases similar to yours.

Advanced out-of-the-box PTAB and TTAB analytics are always at your fingertips.

API

Docket Alarm offers a powerful API (application programming interface) to developers that want to integrate case filings into their apps.

LAW FIRMS
Build custom dashboards for your attorneys and clients with live data direct from the court.

Automate many repetitive legal tasks like conflict checks, document management, and marketing.

FINANCIAL INSTITUTIONS
Litigation and bankruptcy checks for companies and debtors.

E-DISCOVERY AND LEGAL VENDORS
Sync your system to PACER to automate legal marketing.